AGU PUBLICATIONS

JGR

Journal of Geophysical Research: Oceans

RESEARCH ARTICLE

10.1002/2016JC012458

Key Points:
- The fresher/wetter LIA relative to the CWP in the western Pacific may have been caused by the retreat of the East Asian Summer Monsoon
- MCA was similar to CWP rather than much warmer than the latter in the western Pacific
- The drier/saltier MCA and CWP may be associated with the variation of the Pacific Walker Circulation

Supporting Information:
- Supporting Information S1
- Data Set S1

Correspondence to:
W. Deng,
wfdeng@gmail.com,
wfdeng@gig.ac.cn

Citation:
Deng, W., X. Liu, X. Chen, G. Wei, T. Zeng, L. Xie, and J.-X. Zhao (2017), A comparison of the climates of the Medieval Climate Anomaly, Little Ice Age, and Current Warm Period reconstructed using coral records from the northern South China Sea, *J. Geophys. Res. Oceans*, *122*, 264–275, doi:10.1002/2016JC012458.

Received 10 OCT 2016
Accepted 26 NOV 2016
Accepted article online 21 DEC 2016
Published online 17 JAN 2017

A comparison of the climates of the Medieval Climate Anomaly, Little Ice Age, and Current Warm Period reconstructed using coral records from the northern South China Sea

Wenfeng Deng [1], Xi Liu [1,2], Xuefei Chen [1], Gangjian Wei [1], Ti Zeng [3], Luhua Xie [3], and Jian-xin Zhao [4]

[1]State Key Laboratory of Isotope Geochemistry, Guangzhou Institute of Geochemistry, Chinese Academy of Sciences, Guangzhou, China, [2]School of Earth Science, University of Chinese Academy of Sciences, Beijing, China, [3]Key Laboratory of Marginal Sea Geology, Guangzhou Institute of Geochemistry, Chinese Academy of Sciences, Guangzhou, China, [4]Radiogenic Isotope Laboratory, Centre for Microscopy and Microanalysis, The University of Queensland, Brisbane, Queensland, Australia

Abstract For the global oceans, the characteristics of high-resolution climate changes during the last millennium remain uncertain because of the limited availability of proxy data. This study reconstructs climate conditions using annually resolved coral records from the South China Sea (SCS) to provide new insights into climate change over the last millennium. The results indicate that the climate of the Medieval Climate Anomaly (MCA, AD 900–1300) was similar to that of the Current Warm Period (CWP, AD 1850-present), which contradicts previous studies. The similar warmth levels for the MCA and CWP have also been recorded in the Makassar Strait of Indonesia, which suggests that the MCA was not warmer than the CWP in the western Pacific and that this may not have been a globally uniform change. Hydrological conditions were drier/saltier during the MCA and similar to those of the CWP. The drier/saltier MCA and CWP in the western Pacific may be associated with the reduced precipitation caused by variations in the Pacific Walker Circulation. As for the Little Ice Age (LIA, AD 1550–1850), the results from this study, together with previous data from the Makassar Strait, indicate a cold and wet period compared with the CWP and the MCA in the western Pacific. The cold LIA period agrees with the timing of the Maunder sunspot minimum and is therefore associated with low solar activity. The fresher/wetter LIA in the western Pacific may have been caused by the synchronized retreat of both the East Asian Summer Monsoon and the Australian Monsoon.

1. Introduction

Global warming remains an ongoing concern for the climate change research community. To better understand the present-day climate conditions and the potential trends of future climate change, it is necessary to extend the temporal scale of investigation into the last millennium [*Jones et al.*, 1998; *McGregor et al.*, 2015]. The last millennium includes three distinct climate intervals: the Medieval Climate Anomaly (MCA, AD 900–1300) [*Lamb*, 1965; *Crowley and Lowery*, 2000], the Little Ice Age (LIA, AD 1550–1850) [*Robock*, 1979; *Bradley and Jones*, 1993], and the Current Warm Period (CWP, AD 1850–present) [*Wu et al.*, 2012; *Fleury et al.*, 2015]. The MCA and LIA are climate anomalies that were caused by natural forcing (e.g., solar variability and volcanic emissions), but the CWP is linked to anthropogenic factors (e.g., industrialization and land-use changes) [*Masson-Delmotte et al.*, 2013].

A comparison of the climatic and environmental changes that occurred during these three periods is essential if we are to develop a better understanding of past climate change and future global warming. However, instrumental observations cover only the last few decades, and this is clearly insufficient to examine changes that occurred many hundreds of years ago. Therefore, we must extend the historical records by using proxy data [*Mann*, 2002]. A large number of studies based on climate proxies, derived from archives such as coral, foraminifera, mollusks, stalagmites, sediments, tree rings, ice cores, and documentary records, have been used to successfully reconstruct the characteristics of climate change during the three periods defined above [*Jones et al.*, 2009]. Even so, the full characteristics of the seasonal to annual climate during

these periods remain a topic for debate because of the limited availability of proxy data and, in particular, the lack of high-resolution ocean and tropical records [*Yan et al*., 2015a].

The oceans play an integral role in influencing the climate system and are intrinsically linked to the atmosphere through heat storage, transportation of heat around the globe, evaporation, freezing and thawing in polar regions, and gas storage and exchange (including CO_2) [*Herr and Galland*, 2009]. Therefore, obtaining climate change records from the oceans would undoubtedly benefit our understanding of the evolution of the Earth's climate. Massive corals are some of the most reliable sources of proxies used to reconstruct climatic and environmental records from the oceans as these corals incorporate isotope and elemental tracers during the growth of their skeletons that reflect the ambient environmental conditions [*Lough*, 2010]. In addition, they contain clear annual bands and have high growth rates, thereby providing high-resolution and dateable climate information from the surrounding seawater in which they lived [*Gagan et al*., 2000; *Lough*, 2010]. Sr/Ca ratios in coral skeletons have long been used to reconstruct changes in sea surface temperature (SST) [*Smith et al*., 1979], and $\delta^{18}O$ values in coral reflect SST and $\delta^{18}O$ in the ambient seawater [*Swart and Coleman*, 1980]. Residual $\delta^{18}O$ (i.e., $\Delta\delta^{18}O$), which is calculated by subtracting the contribution of temperature from coral $\delta^{18}O$, can be used as a tracer of seawater $\delta^{18}O$ ($\delta^{18}O_{sw}$) and therefore salinity [*Mcculloch et al*., 1994; *Gagan et al*., 2000; *Duprey et al*., 2012]. Many studies have obtained useful records from corals spanning the MCA, LIA, and CMP [*Kuhnert et al*., 2002; *Cobb et al*., 2003; *Zinke et al*., 2015].

As the largest marginal sea of the western tropical Pacific, the climate in the South China Sea (SCS) is controlled by both the East Asian Monsoon and the El Niño-Southern Oscillation over seasonal and interannual timescales, respectively [*Yan et al*., 2011]. Therefore, climate records from the SCS are important in obtaining a better understanding of these climate systems in the past. High-resolution proxy records covering the MCA, LIA, and CWP are very limited, but some composite records from corals, giant clams, ostracod shells, and lake sediments have been used to reconstruct SST and hydrological records from the SCS [*Yan et al*., 2011, 2015a]. The only composite SST record from the SCS that covers the three periods of interest here is based on data from different proxy archives (coral and *Tridacna gigas*) from different periods and different places (the Leizhou Peninsula and Xisha Islands, which are about 500 km apart, with a latitude difference of 1° and longitude difference of 3°) [*Yan et al*., 2015a]; naturally, the uncertainties caused by these differences should not be ignored. In addition, these records cover only about 10 years and therefore do not preserve a complete record of the periods of interest. There is also only one hydrological record from the last millennium from the SCS and this is based on lake sediments and ostracod shells [*Yan et al*., 2011]. Thus, to better understand and consolidate SST data and hydrological information during the three important intervals (the MCA, LIA, and CWP), additional proxy records are required for further validation. This study uses coupled Sr/Ca and $\delta^{18}O$ data from five corals that grew during the MCA, LIA, and CWP to reconstruct the sea surface water conditions, including SST and hydrological changes, from Qionghai, on eastern Hainan Island in the northern SCS. The data from the three important climate periods are then compared, and provide better constraints on past climate variability in the region and this can contribute to refining global climate models that project future climate.

2. Materials and Methods

One modern coral and four fossil coral cores were extracted using an underwater pneumatic drill from five *Porites lutea* colonies, with the diameters of about 0.5–1.5 m, from the water depths of about 4–6 m on the fringing reefs at Qionghai. The modern coral 11LW4 and the fossil coral 11LW2 were collected at Longwan (11LW4: 19°17′11.94″N, 110°39′21.06″E; 11LW2: 19°17′18.84″N, 110°39′23.40″E) in April 2011. The fossil corals 11QG1 and 11QG3 were collected from Qingge (11QG1: 19°18′30.48″N, 110°40′2.46″E; 11QG3: 19°18′3.72″N, 110°39′41.52″E), also in April 2011. The fossil coral 13OC4 was collected from Oucun (19°19′11.22″N, 110°41′31.26″E) in August 2013. The sampling locations are shown in Figure 1. The modern coral 11LW4 was used previously to study decadal variability in the northern SCS [*Deng et al*., 2013; *Chen et al*., 2015; *Wei et al*., 2015].

The four fossil corals were U-Th dated using multicollector inductively coupled plasma mass spectrometers (MC-ICP-MS) at the Radiogenic Isotope Laboratory of the University of Queensland and the High-precision Mass Spectrometry and Environment Change Laboratory of the National Taiwan University. Details of the analytical methods are described by *Zhou et al*. [2011].

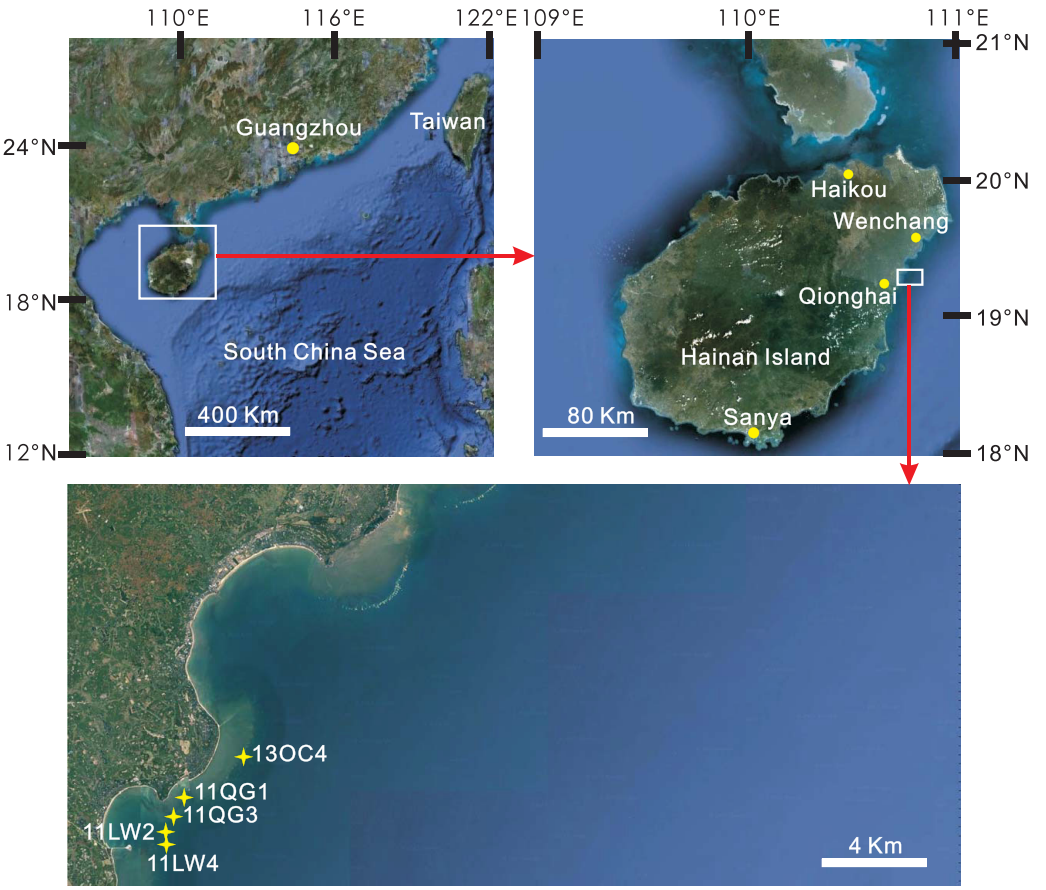

Figure 1. Satellite image of Hainan Island. Yellow stars indicate sampling locations.

The coral cores were first sectioned into slices 1 cm thick and 5–7 cm wide. Then, X-ray photographs were taken to reveal the regular and well-defined annual density bands, which were used to establish the coral chronology. The X-radiographs of the coral 11LW4 refer to *Chen et al.* [2015], and those of other corals are presented in supporting information Figure S1. Next, the coral slices were soaked in 10% H_2O_2 for 24 h to remove organic matter, and this was followed by ultrasonic cleaning in deionized water for 30 min to remove surface contaminates. Samples were collected from annual bands along the main growth axis using a digitally controlled milling machine. Each high-density and low-density band constitutes an annual couplet, generally representing 1 year of growth [*Knutson et al.*, 1972]. X-ray diffraction (XRD) analysis of the samples showed that the coral skeleton was 100% aragonite. Scanning electron microscopy (SEM) imaging revealed that there was no secondary aragonite present in the coral skeleton.

Coral skeletal $\delta^{13}C$ and $\delta^{18}O$ analysis were performed using a GV Isoprime II stable isotope ratio mass spectrometer (IRMS) coupled with a MultiPrep carbonate device that used 102% H_3PO_4 at 90°C to extract CO_2 from the coral samples, following the procedures described by *Deng et al.* [2009]; the IRMS was located at the State Key Laboratory of Isotope Geochemistry, Guangzhou Institute of Geochemistry, Chinese Academy of Sciences, Guangzhou, China. Isotope data were normalized to Vienna Pee Dee Belemnite (V-PDB) using the NBS-19 standard ($\delta^{13}C = 1.95‰$, $\delta^{18}O = -2.20‰$). Multiple measurements on this standard yielded a reproducibility of 0.03‰ for $\delta^{13}C$ and 0.06‰ for $\delta^{18}O$. Replicate measurements were made on approximately 15% of the samples.

Analysis of the Sr/Ca ratios was conducted on a Varian Vista Pro inductively coupled plasma atomic emission spectrometer (ICP-AES), in the same laboratory as that used for the stable isotope measurements. The standard reference material used for the calibration was the JCp-1 *Porites* sp. standard prepared by the Geological Survey of Japan [*Okai et al.*, 2002]. All Sr/Ca data were normalized to JCp-1 with Sr/Ca = 8.838 mmol

mol^{-1} [*Hathorne et al.*, 2013]. Replicate analyses of an in-house *Porites* sp. coral standard solution BH-7 showed excellent reproducibility, with an external precision of 0.16% yielding an SST error of less than 0.5°C.

Coral $\Delta\delta^{18}O$, a tracer for $\delta^{18}O_{sw}$, was calculated by subtracting the sea surface temperature (SST) contribution from the coral $\delta^{18}O$ values [*Gagan et al.*, 2000], according to $\Delta\delta^{18}O = d\delta^{18}O/dT \times [T_{\delta 18O} - T_{Sr/Ca}]$, where $d\delta^{18}O/dT$ is the slope of the empirical $\delta^{18}O$-SST function reported by *Song et al.* [2006], and $T_{\delta 18O}$ and $T_{Sr/Ca}$ are the apparent SSTs calculated from the $\delta^{18}O$ values and Sr/Ca ratios, respectively. We used the Sr/Ca-SST relationship reported by *Gagan et al.* [2012]. This equation has been corrected for the apparent attenuation effect from the skeletal mass accumulation of coral. It is consistent with the calibration determined using the annually resolved Sr/Ca ratios and instrumental SST records from the Great Barrier Reef [*Deng et al.*, 2014]; thus, it is suitable for calculating SST from annually resolved Sr/Ca ratios. According to the error estimation method suggested by *Cahyarini et al.* [2008], the error for the $\Delta\delta^{18}O$ results is about 0.09‰ in this study.

For comparison with coral records, the average annual SST value of 26.0°C for the period 1870–2011 was calculated by averaging the monthly SST values extracted from the HadISST1.1 data set [*Rayner et al.*, 2003] (http://coastwatch.pfeg.noaa.gov/erddap/griddap/erdHadISST.html) for a 1° × 1° grid centered on 19.5°N, 111.5°E (ca. 90 km from the sampling sites). There are no long-term in situ instrumental SST data spanning the whole growth period of the modern coral 11LW4 available. Instrumental records indicate that the average annual SST between 1960 and 1997 was 25.8°C at Qinglan Harbor Meteorological Observatory, which is approximately 35 km from the sample sites used in this study. To assess the effects of the natural forcing on SST and $\delta^{18}O_{sw}$ variability, some data sets were employed for comparison analysis. The total solar irradiance (TSI) data covering the period AD 1000–2003 was reconstructed using a physical model (http://vizier.cfa.harvard.edu/viz-bin/VizieR?-source=J/A+A/531/A6) [*Vieira et al.*, 2011]. Volcanic activity was indicated by the global volcanic aerosol forcing and the smaller forcing corresponds to stronger volcanic eruption [*Sigl et al.*, 2015].

3. Results

Coral samples 11QG1, 11QG3, 11LW2, and 13OC4 were dated to 756 ± 10 year BP, 929 ± 24 year BP, 371 ± 18 year BP, and 254 ± 4 year BP, respectively (Table 1). The ages of these fossil corals (11QG1, 11QG3, 11LW2, and 13OC4) were converted into Common Era years, and their approximate growing intervals were AD 1129–1255, AD 1063–1087, AD 1628–1657, and AD 1702–1772, respectively. Including the modern coral 11LW4, these samples cover the MCA (11QG1 and 11QG3), LIA (11LW2 and 13OC4), and CWP (11LW4).

The average annual SST values reconstructed from the coral Sr/Ca records were 26.5°C ($1\sigma = 0.8$) (MCA), 25.1°C ($1\sigma = 0.8$) (LIA), and 26.6°C ($1\sigma = 1.2$) (CWP) (Figure 2a). The difference of the average annual SST values during the MCA and the CWP was not statistically significant at the significance level of 0.05 ($t = 0.943$, $df = 309$, $p = 0.173$). However, the annual SST value during the LIA was statistically significantly lower than those during the MCA and the CWP at the significance level of 0.05 ($t = -13.9$, $df = 251$, $p < 0.00001$ for LIA and MCA; $t = -11.5$, $df = 258$, $p < 0.00001$ for LIA and CWP).

The average annual $\delta^{18}O_{sw}$ values reconstructed from coral Sr/Ca records and $\delta^{18}O$ were 0.50‰ ($1\sigma = 0.2$) (MCA), 0.12‰ ($1\sigma = 0.2$) (LIA), and 0.40‰ ($1\sigma = 0.3$) (MWP) (Figure 2b). The difference (0.10‰) of the

Table 1. MC-ICP-MS U-Th Dating Results for the Fossil Corals

Sample Name	U (ppm)	±2σ	^{232}Th (ppb)	±2σ	^{230}Th/^{232}Th	±2σ	^{230}Th/^{238}U	±2σ	^{234}U/^{238}U	±2σ	Uncorrected ^{230}Th age (a)	±2σ	Corrected ^{230}Th age (a)	±2σ	Initial ^{234}U/^{238}U	±2σ
11QG1[a]	2.4653	0.0020	1.732	0.007	189.8	1.40	0.008077	0.000052	1.1461	0.0013	772.2	5.1	756	10	1.1464	0.0013
11QG3[a]	2.8684	0.0025	20.052	0.017	26.90	0.42	0.011391	0.000173	1.1464	0.0015	1090.3	16.7	929	24	1.1467	0.0015
11LW2[a]	2.6722	0.0023	14.499	0.013	15.80	0.41	0.005192	0.000134	1.1458	0.0014	495.9	12.9	371	18	1.1459	0.0014
13OC4[b]	2.6771	0.0009	0.247	0.001	88.31	1.26	0.002687	0.000037	1.1449	0.0015	256.6	3.5	254	4	1.1450	0.0015

Ratios are activity ratios calculated from atomic ratios using decay constants of *Cheng et al.* [2000]. All values have been corrected for laboratory procedural blanks. Uncorrected ^{230}Th age (a) was calculated using Isoplot/EX 3.0 program [*Ludwig*, 2003], where a denotes year.

[a]Dates determined in the High-precision Mass Spectrometry and Environment Change Laboratory, National Taiwan University.

[b]Dates determined in the Radiogenic Isotope Laboratory, The University of Queensland.

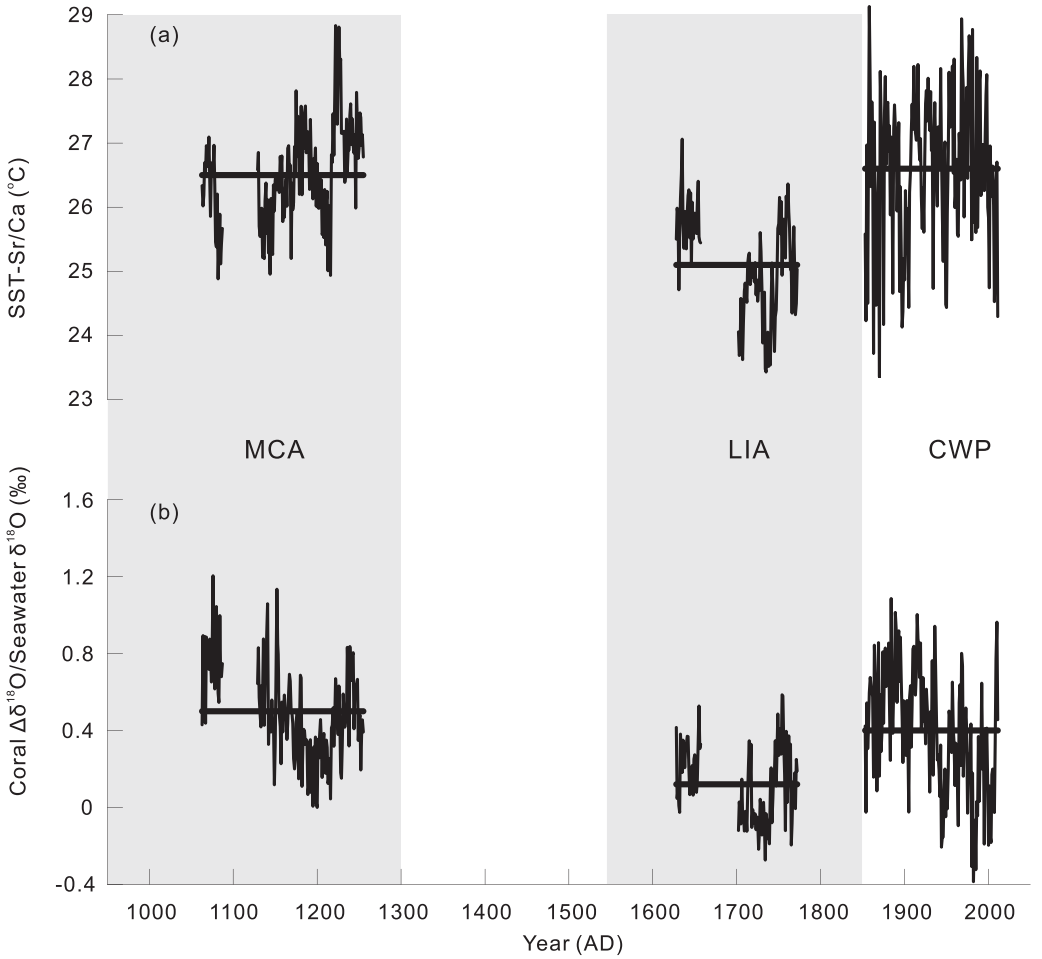

Figure 2. Temporal variations of: (a) SST inferred from coral Sr/Ca time series, and (b) $\delta^{18}O_{sw}$ reconstructed from paired coral Sr/Ca and $\delta^{18}O$ time series during the MCA, LIA, and CWP. Black horizontal lines indicate the averages of SST and $\delta^{18}O_{sw}$ for different periods. The grey vertical bars highlight the borders of different periods.

average annual $\delta^{18}O_{sw}$ values during the MCA and the CWP was statistically significant at the significance level of 0.05 ($t = 2.93$, $df = 309$, $p = 0.002$), but very close to the error of 0.09‰ for the coral $\Delta\delta^{18}O$. However, the annual $\delta^{18}O_{sw}$ value during the LIA was statistically significantly lower than those during the MCA and the CWP at the significance level of 0.05 ($t = -13.0$, $df = 251$, $p < 0.00001$ for LIA and MCA; $t = -8.05$, $df = 258$, $p < 0.00001$ for LIA and CWP).

4. Discussion

4.1. The Applicability of the Coral Records

Our study sites are exactly located in the areas affected by the summer upwelling system along the northeast coasts of Hainan Island [*Jing et al.*, 2009], and the deep ocean water with an unusual Sr/Ca ratio may lead to an artifact in the Sr/Ca-SST calibration [*de Villiers et al.*, 1994]. Therefore, a direct comparison of the coral-derived SST with instrumental data is difficult because there are no long-term in situ data available and gridded data sets smooth out the upwelled cold water SST signal [*Liu et al.*, 2013]. Fortunately, the Sr/Ca-SST equation used here was based on the *Porites* corals from coastal upwelling area and laboratory culturing experiments and has been corrected for the attenuation effect by skeletal mass accumulation [*Gagan et al.*, 2012]. Therefore, it is reliable to act as a bridge to compare the SST difference between different time periods. On the other hand, the average annual SST value for the period 1853–2011 reconstructed from this study's coral Sr/Ca records was 26.6°C, which is close to those of the gridded data (26.0°C) and the instrumental records (25.8°C) nearby. Therefore, taking possible error-inducing factors, including site differences,

errors in the gridded data, instrumental error, and error associated with the SST reconstruction, into consideration, it is believed that the long-term SST records derived from the coral Sr/Ca records generated in this study are reliable. In addition, all coral Sr/Ca data were normalized to the value of the JCp-1 international coral standard, and then converted into SST records using the same Sr/Ca-SST thermometer. In summary, this data supports the idea that the long-term annual average SST values reconstructed here are suitable for comparing and discussing the SST differences between the different periods.

There are no long-term in situ instrumental $\delta^{18}O_{sw}$ data available that span the growth period of the modern coral 11LW4. Gridded data or data from nearby locations are also unavailable. Therefore, it is difficult to discuss the absolute values of the reconstructed $\delta^{18}O_{sw}$. However, the $\delta^{18}O_{sw}$ data extracted from the coral Sr/Ca and $\delta^{18}O$ records are a good proxy for the sea surface salinity (SSS) around Hainan Island in the northern SCS, and have been used to compare the modern-day and mid-Holocene environments [*Guo et al*., 2016]. On the other hand, the $\delta^{18}O_{sw}$ data from the MCA, LIA, and CWP periods are based on the same transfer equations and the same reference standards that the Sr/Ca and $\delta^{18}O$ data were normalized to, which makes it possible to study and compare the relative changes in $\delta^{18}O_{sw}$ and hydrological conditions among the three periods.

4.2. Sea Surface Conditions During the MCA

4.2.1. SST

A high-resolution SST record reconstructed from a *Tridacna gigas* Sr/Ca profile by *Yan et al*. [2015a] suggested that the annual average SST was approximately 0.89°C higher at around AD 990 ± 40 (during the MCA) than that of the present day (Figure 3a). However, the coral records from this study suggest that the long-term annual SST over the periods AD 1161–1287 and AD 1063–1087 during the MCA was about 26.5°C, which is very close to 26.6°C (Figure 2a), the average value of the long-term annual SST during the CWP. This difference between the MCA and CWP based on coral records is similar to that indicated from the reconstructed surface temperature pattern in Figure 2 of *Mann et al*. [2009]. The inconsistency between reconstructed SST results from these coral records and the previous *Tridacna gigas* record of *Yan et al*. [2015a] may result from the different timespans over which the proxies grew. On the other hand, the record analyzed by *Yan et al*. [2015a] may be too short to represent the situation of the overall period. There are no alternative high-resolution SST records from the MCA for comparison in the northern SCS, but the records from foraminifera Mg/Ca suggest that the average SST during the period AD 1000–1400 (the MCA) was very similar to that of the CWP in the Makassar Strait of Indonesia, in the tropical Indo-Pacific warm pool [*Newton et al*., 2006; *Oppo et al*., 2009]. At the same time, the annual variations in SST obtained from coral Sr/Ca and foraminifera Mg/Ca are very similar (Figures 3b and 3c). An SST record reconstructed from tetraether lipids recovered from planktonic archaea indicates an analog or even a colder MCA relative to the CWP in the southern Okinawa Trough, in the western Pacific [*Wu et al*., 2012].

The Medieval Solar Maximum coincides roughly with the MCA [*Jirikowic and Damon*, 1994], and the causes of the MCA have been linked to increased solar activity, decreased volcanism, and ocean-atmosphere interactions [*Hughes and Diaz*, 1994]. To assess the effects of the natural forcing on SST variability during these periods, we compared proxies for these forcing factors with our reconstructed SST record. For example, the variations in the TSI roughly matched those of the SST records (Figure 3d), which may mean that the variations in SST mainly responded to forcing by solar irradiance. However, the variations in global volcanic aerosol forcing did not match those of the SST record (Figure 3e), which may mean that the effect of volcanic activity on SST was limited in the study area. The roles of ocean-atmosphere interactions were not discussed here since there was no appropriate proxy available.

A recent study based on foraminifera Mg/Ca shows that the MCA was global in scope [*Rosenthal et al*., 2013], but most previous studies pointed out that the existence of the MCA in the Southern Hemisphere is uncertain and it was not a global event [*Hughes and Diaz*, 1994; *Crowley and Lowery*, 2000]. Regarding the amplitude of the MCA, some Northern Hemisphere temperature reconstructions support the interpretation that the MCA was at most comparable with the mid-20th century Northern Hemisphere temperature peak and about 0.3°C cooler than the decadal average of the 1990s [*Jones et al*., 1998; *Mann et al*., 1999]. On the other hand, because of uncertainties associated with the proxy-instrumental temperature calibration, there is no robust evidence to support the conclusion that the MCA was warmer than the CWP [*Crowley and Lowery*, 2000]. The records from this study are based on the same proxy and they were normalized to the

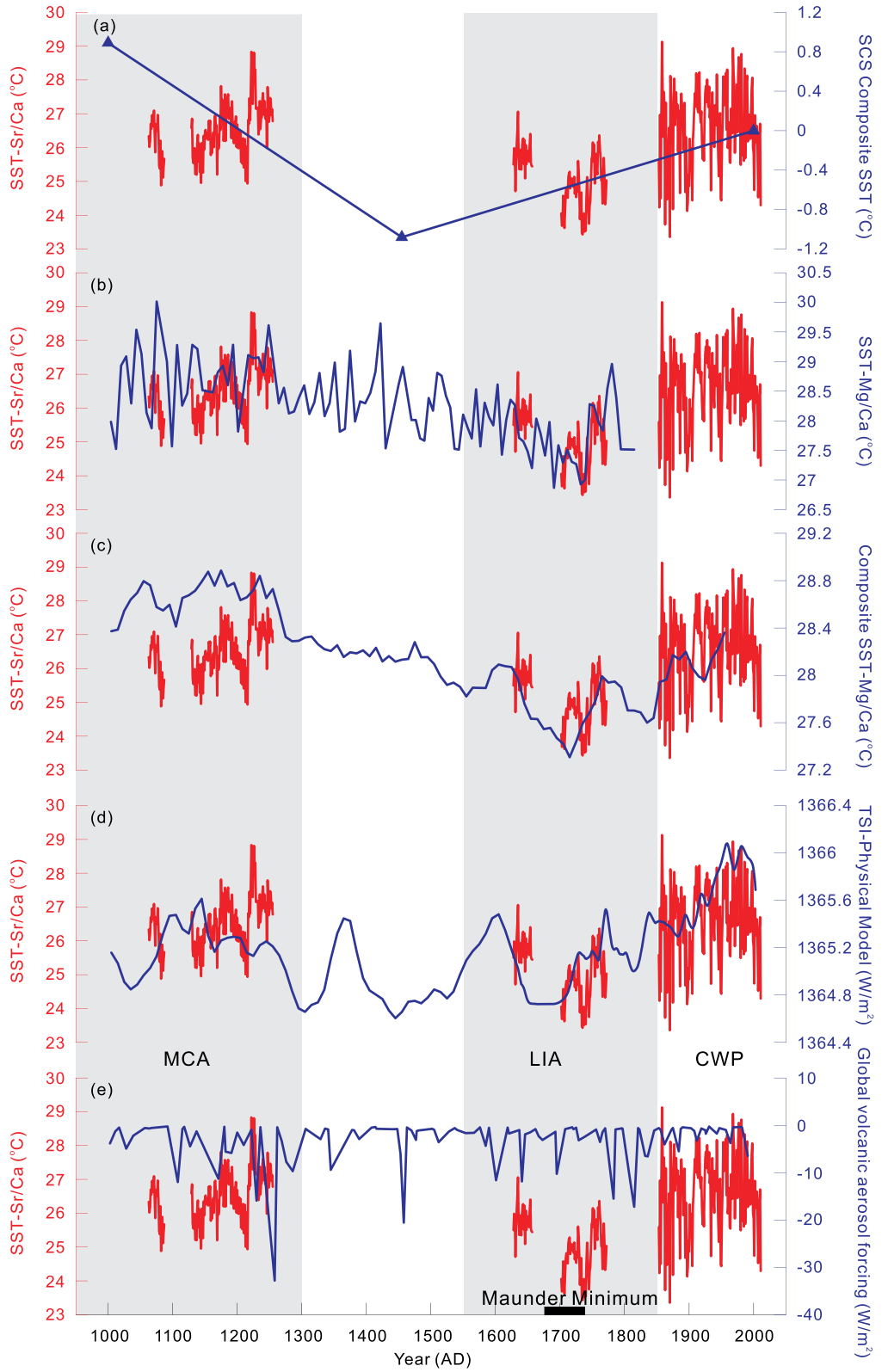

Figure 3. Comparison of SST records based on coral Sr/Ca time series from the northern SCS (red lines) with the (a) composite SST records from coral and *Tridacna gigas* in the SCS [*Yan et al.*, 2015a], (b) SST records reconstructed from foraminiferal Mg/Ca profiles in a single sediment core from the Makassar Strait of Indonesia [*Newton et al.*, 2006], (c) SST records from composite foraminiferal Mg/Ca ratios in the Makassar Strait of Indonesia [*Oppo et al.*, 2009], (d) TSI using a physical model [*Vieira et al.*, 2011], and (e) global volcanic aerosol forcing [*Sigl et al.*, 2015]. Blue lines indicate the other variables. The grey vertical bars denote the MCA and LIA. The black horizontal bar denotes the Maunder Minimum.

same reference standard; consequently, they should record the difference between the MCA and CWP accurately. Therefore, the results of this work from the northern SCS, together with those from the tropical Indo-Pacific warm pool, demonstrate that the MCA was similar to the CWP, rather than much warmer than it, in the western Pacific, and that the MCA may not have been a globally uniform change.

4.2.2. $\delta^{18}O_{sw}$

The average value of the MCA $\delta^{18}O_{sw}$ is about 0.10‰ higher than that of the CWP $\delta^{18}O_{sw}$. The positive $\delta^{18}O_{sw}$ difference seems to suggest a slightly higher SSS during the MCA and a slightly drier MCA relative to the CWP. However, compared with the error of approximately 0.09‰ for the coral $\Delta\delta^{18}O$ results, this difference of 0.10‰ is very close to their estimated errors. Therefore, it is suggested that hydrological conditions during the CWP were similar to those of the MCA. However, a study based on geochemical proxies in sediments from Lake Huguangyan, in tropical south China, indicated a much drier climate during the MCA compared with the CWP [*Chu et al.*, 2002]. Even so, the conclusion of this study that hydrological conditions were similar during the MCA and CWP is consistent with findings from the tropical Indo-Pacific warm pool. Drier and saltier hydrographic conditions were inferred from foraminiferal Mg/Ca and $\delta^{18}O$ time series for the MCA in the tropical Indo-Pacific warm pool, but this is similar to the present-day conditions (Figures 4a and 4b) [*Newton et al.*, 2006; *Oppo et al.*, 2009]. The differences in the variation trends obtained from the coral and foraminiferal records (Figures 4a and 4b) may be related to dating errors between the two proxies.

Therefore, the results from the northern SCS in this study, together with the results from the tropical Indo-Pacific warm pool, indicate similar hydrological conditions during the MCA and CWP in the western Pacific. Compared with the wet LIA, the drier/saltier conditions during the MCA and CWP may have been caused by the reduced precipitation levels associated with variations in the Pacific Walker Circulation over the last millennium [*Yan et al.*, 2011]. However, this mechanism should be further studied using numerical simulations and theoretical analysis.

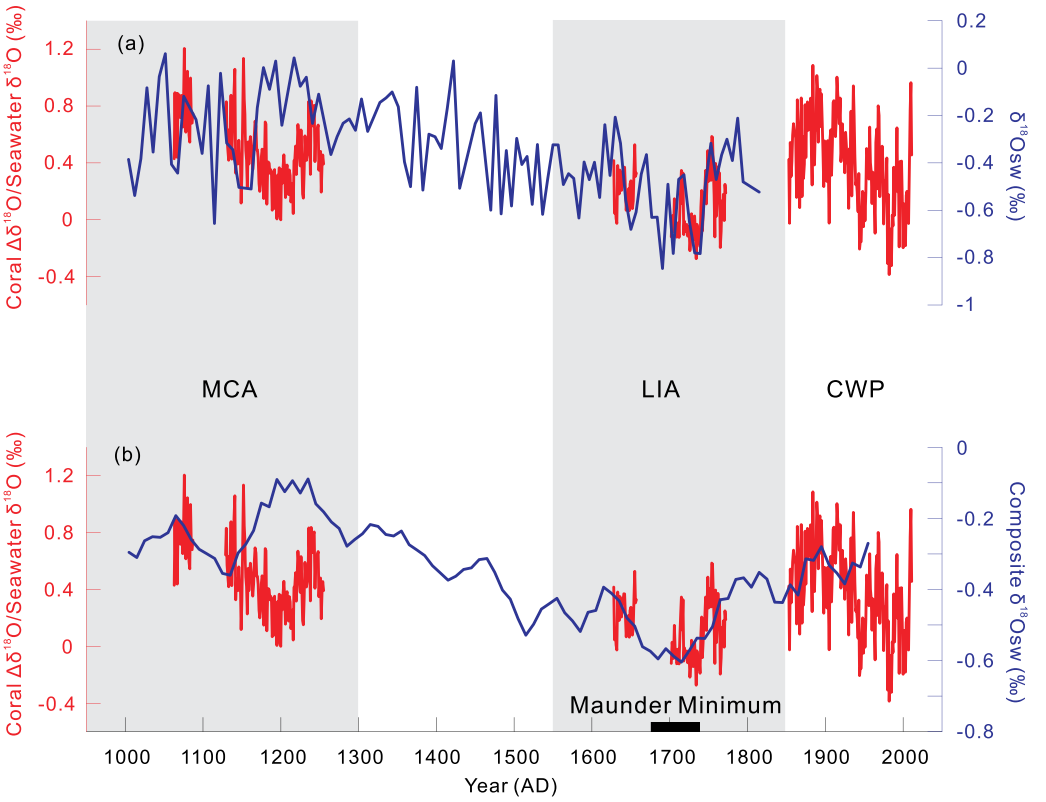

Figure 4. Comparison of $\delta^{18}O_{sw}$ records based on coral Sr/Ca and $\delta^{18}O$ time series from the northern SCS (red lines) and reconstructed from foraminiferal Mg/Ca and $\delta^{18}O$ profiles in (a) a single sediment core [*Newton et al.*, 2006] and (b) multicores [*Oppo et al.*, 2009] from the Makassar Strait of Indonesia (blue lines). The grey vertical bars denote the MCA and LIA. The black horizontal bar indicates the Maunder Minimum.

4.3. Sea Surface Conditions During the LIA

4.3.1. SST

Previous studies support the opinion that the 15th to 19th centuries were the coldest of the millennium in the Northern Hemisphere, but this LIA can only be considered to be a modest cooling (<1°C) relative to late 20th century levels [*Bradley and Jones*, 1993; *Jones et al*., 1998; *Mann et al*., 1999]. The Intergovernmental Panel on Climate Change's Fifth Assessment Report also suggested that the LIA represents independent regional climate change, rather than a globally synchronous increase in glaciation, and at most there was only modest cooling of the Northern Hemisphere during this period [*Masson-Delmotte et al*., 2013]. However, recent studies have found evidence of the LIA in the Southern Hemisphere and support the concept of a global LIA [*Rosenthal et al*., 2013].

There is only one high-resolution SST record for the LIA reconstructed from coral Sr/Ca, and this indicates that the annual SST around AD 1455 $\pm$ 51 was about 1.08°C lower than that of the present day in the northern SCS (Figure 3a) [*Yan et al*., 2015a]. The coral records generated in this study suggest that the average of the long-term annual SST over the periods AD 1628–1657 and AD 1702–1772 was about 1.5°C lower than that during the CWP, which is within the range of 1–3°C cooler relative to the CWP in the northern SCS indicated by the reconstructed surface temperature pattern shown in Figure 2 of *Mann et al*. [2009]. These cooling amplitudes from the northern SCS are also comparable with those from other sites. For example, in the Pacific Ocean, foraminifera Mg/Ca records indicate that SSTs during the LIA were 0.5–1.5°C lower than during the CWP in the Makassar Strait of Indonesia, in the tropical Indo-Pacific warm pool (Figures 3b and 3c) [*Newton et al*., 2006; *Oppo et al*., 2009], and a record derived from coral Sr/Ca and U/Ca suggests that the LIA SSTs were, on average, 1.4°C lower than during the past 30 years in New Caledonia in the southwest tropical Pacific [*Corrège et al*., 2001]. Other records from coral δ^{18}O, Mg/Ca, and Sr/Ca in the Atlantic indicate that SSTs during the LIA were 1.5–2.0°C lower than during the CWP [*Watanabe et al*., 2001; *Goodkin et al*., 2005]. Like the situation during the MCA, these results are also in good agreement with that of *Newton et al*. [2006], who found that LIA SSTs were 1.5°C cooler in the Makassar Strait. At the same time, the SST profiles extracted from foraminifera Mg/Ca and coral Sr/Ca time series are very similar (Figures 3b and 3c). The coldest period was centered around AD 1680–1730, which is consistent with the findings of *Monroe and Wicander* [2009]. The LIA SSTs gradually decreased before the coldest phase, and after that, SSTs increased gradually. This coldest phase (AD 1680–1730) coincided with the Maunder sunspot minimum [*Sicre et al*., 2008], and the Maunder Minimum from AD 1680 to AD 1730 was a period of almost no sunspots [*Serreze and Barry*, 2014]. Therefore, the coral Sr/Ca record produced in this study, together with data from foraminifera Mg/Ca time series, may indicate that the LIA was a synchronous cool period across the western Pacific, and its maximum was probably associated with solar activity [*Rind et al*., 2004]. As mentioned above discussion for the MCA SST records, the cause of the LIA might be mainly associated with solar irradiance, and roles of volcanic activity were limited (Figures 3d and 3e). However, it may have been triggered by volcanism and sustained by sea ice and/or ocean feedbacks [*Miller et al*., 2012].

4.3.2. $\delta^{18}O_{sw}$

The average $\delta^{18}O_{sw}$ value of the LIA is about 0.28‰ lower than that of the CWP, and this difference in $\delta^{18}O_{sw}$ corresponds to a difference of about 1.5 in SSS as estimated using the SSS-$\delta^{18}O_{sw}$ relationship for the northern SCS [*Ye et al*., 2014]. This SSS difference between the LIA and CWP is similar to that reported from the Makassar Strait [*Newton et al*., 2006; *Oppo et al*., 2009], and the $\delta^{18}O_{sw}$ profiles from these two study sites are also similar (Figures 4a and 4b). These results indicate that, during the LIA in the western Pacific, seawater was fresher than that in the CWP and conditions were relatively wet. Although *Wang et al*. [1999] reported drier conditions and a higher SSS during the LIA in the northern SCS, most previous studies have found a wet LIA in tropical south China and the northern SCS [*Yan et al*., 2011; *Zeng et al*., 2012; *Wang et al*., 2013]. Various explanations have been offered regarding the wet LIA in tropical south China and the northern SCS, such as a strengthened, and perhaps more westward, Pacific Walker Circulation [*Yan et al*., 2011], a weakened East Asian summer monsoon caused by reduced solar irradiation [*Zeng et al*., 2012], and elevated precipitation associated with increased solar irradiance [*Wang et al*., 2013]. However, the last two explanations are contradictory. The wet LIA in the Makassar Strait has been linked to the southward movement of the Intertropical Convergence Zone (ITCZ) [*Newton et al*., 2006]. A recent study that integrated multiple records proposed an alternative and more physically plausible hypothesis for the wet LIA over the western Pacific, i.e., a synchronized retreat of both the East Asian Summer Monsoon and the Australian Monsoon, probably driven by reduced solar activity [*Yan et al*., 2015b]. This mechanism can also be used to

explain the wet LIA in the northern SCS. The wettest phase of the LIA found here agrees with that of *Newton et al*. [2006] and is also nearly centered on the Maunder sunspot minimum (AD 1680–1730) (Figure 4). Modeling by *Yan et al*. [2015b] suggests that low solar activity during the LIA may have led to increased rainfall in the equatorial area.

5. Conclusions

Based on geochemical records from coupled Sr/Ca and $\delta^{18}O$ time series preserved in corals whose growing periods covered the MCA, LIA, and CWP, the sea surface conditions, including temperature and hydrological conditions, of the northern SCS were reconstructed for these three climate intervals. The main conclusions are as follows:

1. The average long-term annual SST during the LIA was about 1.5°C lower than that of the CWP in the northern SCS. This difference is similar to that in the tropical Indo-Pacific warm pool, but is a little larger than that found by *Yan et al*. [2015a] using a composite record derived from different proxies. In addition, the SST profile for the LIA derived from the coral Sr/Ca record in this study is also the same as that from the tropical Indo-Pacific warm pool (based on foraminifera Mg/Ca records), which indicates a synchronous LIA in the western Pacific. This cold phase (AD 1680–1730) occurred at the same time as the Maunder sunspot minimum and is therefore likely to have been driven by reduced solar activity.
2. The average LIA $\delta^{18}O_{sw}$ value was about 0.28‰ lower than that of the CWP $\delta^{18}O_{sw}$, and this difference in $\delta^{18}O_{sw}$ corresponds to a difference of about 1.5 in SSS. This SSS difference between the LIA and CWP is similar to that found in the tropical Indo-Pacific warm pool. The fresher and wetter LIA in the western Pacific may have been caused by the synchronized retreat of both the East Asian Summer Monsoon and the Australian Monsoon, which was probably related to reduced solar activity [*Yan et al*., 2015b]. The wettest phase of the LIA was also nearly centered at the Maunder sunspot minimum (AD 1680–1730) and may be linked to an increase in rainfall in the equatorial area during the periods of low solar activity [*Yan et al*., 2015b].
3. In contrast to *Yan et al*. [2015a], who concluded that the MCA was much warmer than the CWP in the northern SCS, the results from the northern SCS generated in this study, together with those from another study in the tropical Indo-Pacific warm pool, demonstrate that MCA was not much warmer than the CWP, but similar to it in the western Pacific, and that the MCA may not have been a globally uniform event.
4. The hydrological conditions were drier and saltier during the MCA, but were similar to those of the CWP. The drier/saltier MCA and CWP in the northern SCS may have been related to reduced precipitation amounts caused by variations in the Pacific Walker Circulation. However, further study is needed to confirm the mechanism.

Acknowledgments

Yi Liu of the University of Science and Technology of China is appreciated for his assistance with U-Th dating measurements in the National Taiwan University. The authors would like to thank the editor Peter G. Brewer and two anonymous reviewers for their helpful comments and constructive suggestions. The English of the manuscript was improved by Stallard Scientific Editing. This work was supported by the National Key Research and Development Project of China (2016YFA0601204 and 2013CB956103), the National Natural Sciences Foundation of China (41673115 and 41325012), and the State Key Laboratory of Isotope Geochemistry (SKLIG-RC-14-02). This is contribution IS-2317 from GIGCAS. The data for this paper are available as the online supporting data set and from the corresponding author Deng (wfdeng@gmail.com, wfdeng@gig.ac.cn).

References

Bradley, R. S., and P. D. Jones (1993), 'Little Ice Age' summer temperature variations: Their nature and relevance to recent global warming trends, *Holocene*, *3*(4), 367–376.

Cahyarini, S. Y., M. Pfeiffer, O. Timm, W. C. Dullo, and D. G. Schonberg (2008), Reconstructing seawater $\delta^{18}O$ from paired coral $\delta^{18}O$ and Sr/Ca ratios: Methods, error analysis and problems, with examples from Tahiti (French Polynesia) and Timor (Indonesia), *Geochim. Cosmochim. Acta*, *72*(12), 2841–2853.

Chen, X. F., G. J. Wei, W. F. Deng, Y. Liu, Y. L. Sun, T. Zeng, and L. H. Xie (2015), Decadal variations in trace metal concentrations on a coral reef: Evidence from a 159 year record of Mn, Cu, and V in a Porites coral from the northern South China Sea, *J. Geophys. Res. Oceans*, *120*, 405–416, doi:10.1002/2014JC010390.

Cheng, H., R. L. Edwards, J. Hoff, C. D. Gallup, D. A. Richards, and Y. Asmerom (2000), The half-lives of uranium-234 and thorium-230, *Chem. Geol.*, *169*(1-2), 17–33.

Chu, G., J. Liu, Q. Sun, H. Lu, Z. Gu, W. Wang, and T. Liu (2002), The 'Mediaeval Warm Period' drought recorded in Lake Huguangyan, tropical South China, *Holocene*, *12*(5), 511–516.

Cobb, K. M., C. D. Charles, H. Cheng, and R. L. Edwards (2003), El Nino/Southern Oscillation and tropical Pacific climate during the last millennium, *Nature*, *424*(6946), 271–276.

Corrège, T., T. Quinn, T. Delcroix, F. Le Cornec, J. Recy, and G. Cabioch (2001), Little Ice Age sea surface temperature variability in the southwest tropical Pacific, *Geophys. Res. Lett.*, *28*(18), 3477–3480.

Crowley, T. J., and T. S. Lowery (2000), How warm was the Medieval Warm Period?, *Ambio*, *29*(1), 51–54.

Deng, W. F., G. J. Wei, X. H. Li, K. F. Yu, J. X. Zhao, W. D. Sun, and Y. Liu (2009), Paleoprecipitation record from coral Sr/Ca and $\delta^{18}O$ during the mid Holocene in the northern South China Sea, *Holocene*, *19*(6), 811–821.

Deng, W. F., G. J. Wei, L. H. Xie, T. Ke, Z. B. Wang, T. Zeng, and Y. Liu (2013), Variations in the Pacific Decadal Oscillation since 1853 in a coral record from the northern South China Sea, *J. Geophys. Res. Oceans*, *118*, 2358–2366, doi:10.1002/jgrc.20180.

Deng, W. F., G. J. Wei, M. McCulloch, L. H. Xie, Y. Liu, and T. Zeng (2014), Evaluation of annual resolution coral geochemical records as climate proxies in the Great Barrier Reef of Australia, *Coral Reefs*, *33*(4), 965–977.
de Villiers, S., G. T. Shen, and B. K. Nelson (1994), The Sr/Ca-temperature relationship in coralline aragonite: Influence of variability in $(Sr/Ca)_{seawater}$ and skeletal growth parameters, *Geochim. Cosmochim. Acta*, *58*(1), 197–208.
Duprey, N., C. E. Lazareth, T. Corrège, F. Le Cornec, C. Maes, N. Pujol, M. Madeng-Yogo, S. Caquineau, C. Soares Derome, and G. Cabioch (2012), Early mid-Holocene SST variability and surface-ocean water balance in the southwest Pacific, *Paleoceanography*, *27*, PA4207, doi: 10.1029/2012PA002350.
Fleury, S., P. Martinez, X. Crosta, K. Charlier, I. Billy, V. Hanquiez, T. Blanz, and R. R. Schneider (2015), Pervasive multidecadal variations in productivity within the Peruvian Upwelling System over the last millennium, *Quat. Sci. Rev.*, *125*, 78–90.
Gagan, M. K., L. K. Ayliffe, J. W. Beck, J. E. Cole, E. R. M. Druffel, R. B. Dunbar, and D. P. Schrag (2000), New views of tropical paleoclimates from corals, *Quat. Sci. Rev.*, *19*(1–5), 45–64.
Gagan, M. K., G. B. Dunbar, and A. Suzuki (2012), The effect of skeletal mass accumulation in Porites on coral Sr/Ca and $\delta^{18}O$ paleothermometry, *Paleoceanography*, *27*, PA1203, doi:10.1029/2011PA002215.
Goodkin, N. F., K. A. Hughen, A. L. Cohen, and S. R. Smith (2005), Record of Little Ice Age sea surface temperatures at Bermuda using a growth-dependent calibration of coral Sr/Ca, *Paleoceanography*, *20*, PA4016, doi:10.1029/2005PA001140.
Guo, Y., W. Deng, X. Chen, G. Wei, K. Yu, and J.-x. Zhao (2016), Saltier sea surface water conditions recorded by multiple mid-Holocene corals in the northern South China Sea, *J. Geophys. Res. Oceans*, *121*, 6323–6330, doi:10.1002/2016JC012034.
Hathorne, E. C., et al. (2013), Interlaboratory study for coral Sr/Ca and other element/Ca ratio measurements, *Geochem. Geophys. Geosyst.*, *14*(9), 3730–3750, doi:10.1002/ggge.20230.
Herr, D., and G. R. Galland (2009), *The Ocean and Climate Change, Tools and Guidelines for Action*, 72 pp., IUCN U.S. Multilateral Off., Gland, Switzerland.
Hughes, M. K., and H. F. Diaz (1994), Was there a 'medieval warm period', and if so, where and when?, *Clim. Change*, *26*(2), 109–142.
Jing, Z.-y., Y.-q. Qi, Z.-l. Hua, and H. Zhang (2009), Numerical study on the summer upwelling system in the northern continental shelf of the South China Sea, *Cont. Shelf Res.*, *29*(2), 467–478.
Jirikowic, J. L., and P. E. Damon (1994), The medieval solar activity maximum, *Clim. Change*, *26*(2), 309–316.
Jones, P. D., K. R. Briffa, T. P. Barnett, and S. F. B. Tett (1998), High-resolution palaeoclimatic records for the last millennium: Interpretation, integration and comparison with General Circulation Model control-run temperatures, *Holocene*, *8*(4), 455–471.
Jones, P. D., et al. (2009), High-resolution palaeoclimatology of the last millennium: A review of current status and future prospects, *Holocene*, *19*(1), 3–49.
Knutson, D. W., S. V. Smith, and R. W. Buddemeier (1972), Coral chronometers: Seasonal growth bands in reef corals, *Science*, *177*(4045), 270–272.
Kuhnert, H., J. Patzold, B. Schnetger, and G. Wefer (2002), Sea-surface temperature variability in the 16th century at Bermuda inferred from coral records, *Paleogeogr. Paleoclimatol. Paleoecol.*, *179*(3–4), 159–171.
Lamb, H. H. (1965), The early medieval warm epoch and its sequel, *Paleogeogr. Paleoclimatol. Paleoecol.*, *1*, 13–37.
Liu, Y., Z. C. Peng, C. C. Shen, R. J. Zhou, S. H. Song, Z. G. Shi, T. Chen, G. J. Wei, and K. L. DeLong (2013), Recent 121-year variability of western boundary upwelling in the northern South China Sea, *Geophys. Res. Lett.*, *40*, 3180–3183, doi:10.1002/grl.50381.
Lough, J. M. (2010), Climate records from corals, *Wiley Interdiscip. Rev. Clim. Change*, *1*(3), 318–331.
Ludwig, K. R., (2003), User's manual for Isoplot/Ex Version 3.0: a geochronological toolkit for Microsoft Excel, Berkeley Geochronology Centre, Special Publication No. 4.
Mann, M. E. (2002), The value of multiple proxies, *Science*, *297*(5586), 1481–1482.
Mann, M. E., R. S. Bradley, and M. K. Hughes (1999), Northern hemisphere temperatures during the past millennium: Inferences, uncertainties, and limitations, *Geophys. Res. Lett.*, *26*(6), 759–762.
Mann, M. E., Z. Zhang, S. Rutherford, R. S. Bradley, M. K. Hughes, D. Shindell, C. Ammann, G. Faluvegi, and F. Ni (2009), Global signatures and dynamical origins of the Little Ice Age and medieval climate anomaly, *Science*, *326*(5957), 1256–1260.
Masson-Delmotte, V., et al. (2013), Information from paleoclimate archives, in *Climate Change 2013: The Physical Science Basis. Contribution of Working Group I to the Fifth Assessment Report of the Intergovernmental Panel on Climate Change*, edited by T. F. Stocker et al., pp. 383–464, Cambridge Univ. Press, Cambridge, U. K.
Mcculloch, M. T., M. K. Gagan, G. E. Mortimer, A. R. Chivas, and P. J. Isdale (1994), A high-resolution Sr/Ca and $\delta^{18}O$ coral record from the Great Barrier Reef, Australia, and the 1982–1983 El-Niño, *Geochim. Cosmochim. Acta*, *58*(12), 2747–2754.
McGregor, H. V., et al. (2015), Robust global ocean cooling trend for the pre-industrial Common Era, *Nat. Geosci.*, *8*(9), 671–677.
Miller, G. H., et al. (2012), Abrupt onset of the Little Ice Age triggered by volcanism and sustained by sea-ice/ocean feedbacks, *Geophys. Res. Lett.*, *39*, L02708, doi:10.1029/2011GL050168.
Monroe, J., and R. Wicander (2009), *The Changing Earth: Exploring Geology and Evolution*, 752 pp., Cengage Learning Press, Australia.
Newton, A., R. Thunell, and L. Stott (2006), Climate and hydrographic variability in the Indo-Pacific Warm Pool during the last millennium, *Geophys. Res. Lett.*, *33*, L19710, doi:10.1029/2006GL027234.
Okai, T., A. Suzuki, H. Kawahata, S. Terashima, and N. Imai (2002), Preparation of a new Geological Survey of Japan geochemical reference material: Coral JCp-1, *Geostand. Newsl.*, *26*(1), 95–99.
Oppo, D. W., Y. Rosenthal, and B. K. Linsley (2009), 2,000-year-long temperature and hydrology reconstructions from the Indo-Pacific warm pool, *Nature*, *460*(7259), 1113–1116.
Rayner, N. A., D. E. Parker, E. B. Horton, C. K. Folland, L. V. Alexander, D. P. Rowell, E. C. Kent, and A. Kaplan (2003), Global analyses of sea surface temperature, sea ice, and night marine air temperature since the late nineteenth century, *J. Geophys. Res.*, *108*(D14), 4407, doi: 10.1029/2002JD002670.
Rind, D., D. Shindell, J. Perlwitz, J. Lerner, P. Lonergan, J. Lean, and C. McLinden (2004), The relative importance of solar and anthropogenic forcing of climate change between the Maunder Minimum and the present, *J. Clim.*, *17*(5), 906–929.
Robock, A. (1979), The "Little Ice Age": Northern Hemisphere average observations and model calculations, *Science*, *206*(4425), 1402–1404.
Rosenthal, Y., B. K. Linsley, and D. W. Oppo (2013), Pacific Ocean heat content during the past 10,000 Years, *Science*, *342*(6158), 617–621.
Serreze, M. C., and R. G. Barry (2014), *The Arctic Climate System*, 442 pp., Cambridge Univ. Press, United States of America.
Sicre, M.-A., J. Jacob, U. Ezat, S. Rousse, C. Kissel, P. Yiou, J. Eiríksson, K. L. Knudsen, E. Jansen, and J.-L. Turon (2008), Decadal variability of sea surface temperatures off North Iceland over the last 2000 years, *Earth Planet. Sci. Lett.*, *268*(1–2), 137–142.
Sigl, M., et al. (2015), Timing and climate forcing of volcanic eruptions for the past 2,500 years, *Nature*, *523*(7562), 543–549.
Smith, S. V., R. W. Buddemeier, R. C. Redalje, and J. E. Houck (1979), Strontium-calcium thermometry in coral skeletons, *Science*, *204*(4391), 404–407.

Song, S. H., W. J. Zhou, Z. C. Peng, W. G. Liu, P. Cheng, and F. Xian (2006), Response to environmental conditions of coral δ^{18}O of *Porites lutea* from Shalao, Hainan Island [in Chinese with English abstract], *Mar. Geol. Quat. Geol.*, *26*(4), 23–28.

Swart, P. K., and M. L. Coleman (1980), Isotopic data for scleractinian corals explain their paleotemperature uncertainties, *Nature*, *283*(5747), 557–559.

Vieira, L. E. A., S. K. Solanki, N. A. Krivova, and I. Usoskin (2011), Evolution of the solar irradiance during the Holocene, *Astron. Astrophys.*, *531*, A6.

Wang, L.-C., H. Behling, T.-Q. Lee, H.-C. Li, C.-A. Huh, L.-J. Shiau, S.-H. Chen, and J.-T. Wu (2013), Increased precipitation during the Little Ice Age in northern Taiwan inferred from diatoms and geochemistry in a sediment core from a subalpine lake, *J. Paleolimn.*, *49*(4), 619–631.

Wang, L. J., M. Sarnthein, H. Erlenkeuser, P. M. Grootes, J. O. Grimalt, C. Pelejero, and G. Linck (1999), Holocene variations in Asian monsoon moisture: A bidecadal sediment record from the South China Sea, *Geophys. Res. Lett.*, *26*(18), 2889–2892.

Watanabe, T., A. Winter, and T. Oba (2001), Seasonal changes in sea surface temperature and salinity during the Little Ice Age in the Caribbean Sea deduced from Mg/Ca and ^{18}O/^{16}O ratios in corals, *Mar. Geol.*, *173*(1–4), 21–35.

Wei, G. J., Z. B. Wang, T. Ke, Y. Liu, W. F. Deng, X. F. Chen, J. F. Xu, T. Zeng, and L. H. Xie (2015), Decadal variability in seawater pH in the West Pacific: Evidence from coral δ^{11}B records, *J. Geophys. Res. Oceans*, *120*, 7166–7181, doi:10.1002/2015JC011066.

Wu, W., W. Tan, L. Zhou, H. Yang, and Y. Xu (2012), Sea surface temperature variability in southern Okinawa Trough during last 2700 years, *Geophys. Res. Lett.*, *39*, L14705, doi:10.11029/2012GL052749.

Yan, H., L. Sun, D. W. Oppo, Y. Wang, Z. Liu, Z. Xie, X. Liu, and W. Cheng (2011), South China Sea hydrological changes and Pacific Walker Circulation variations over the last millennium, *Nat. Commun.*, *2*, 293.

Yan, H., W. Soon, and Y. H. Wang (2015a), A composite sea surface temperature record of the northern South China Sea for the past 2500 years: A unique look into seasonality and seasonal climate changes during warm and cold periods, *Earth Sci. Rev.*, *141*, 122–135.

Yan, H., W. Wei, W. Soon, Z. S. An, W. J. Zhou, Z. H. Liu, Y. H. Wang, and R. M. Carter (2015b), Dynamics of the intertropical convergence zone over the western Pacific during the Little Ice Age, *Nat. Geosci.*, *8*(4), 315–320.

Ye, F., W. Deng, L. Xie, G. Wei, and G. Jia (2014), Surface water δ^{18}O in the marginal China seas and its hydrological implications, *Estuarine Coastal Shelf Sci.*, *147*, 25–31.

Zeng, Y., J. Chen, Z. Zhu, J. Li, J. Wang, and G. Wan (2012), The wet Little Ice Age recorded by sediments in Huguangyan Lake, tropical South China, *Quat. Int.*, *263*, 55–62.

Zhou, H., J. Zhao, W. Qing, Y. Feng, and J. Tang (2011), Speleothem-derived Asian summer monsoon variations in Central China, 54–46 ka, *J. Quat. Sci.*, *26*(8), 781–790.

Zinke, J., A. Hoell, J. M. Lough, M. Feng, A. J. Kuret, H. Clarke, V. Ricca, K. Rankenburg, and M. T. McCulloch (2015), Coral record of southeast Indian Ocean marine heatwaves with intensified Western Pacific temperature gradient, *Nat. Commun.*, *6*, 8562.